Yun, Y.; Hernández Rodríguez, M.; Wan, W.; Zou, X.; Jorda Moret, JL.; Cantin Sanz, A.; Rey Garcia, F.... (2015). The first zeolite with a tri-directional extra-large 14-ring pore system derived using a phosphonium-based organic molecule. Chemical Communications. 51(36):7602-7605. doi:10.1039/c4cc10317c

Journal Name

RSCPublishing

COMMUNICATION

The first zeolite with a tri-directional extra-large 14-ring pore system derived using a phosphonium-based organic molecule

Cite this: DOI: 10.1039/x0xx00000x

Yifeng Yun, [‡a] Manuel Hernández,[‡b] Wei Wan,[a] Xiaodong Zou,[*a] Jose L. Jordá,[b] Angel Cantín,[b] Fernando Rey,[b] Avelino Corma[*b]

Received 00th January 2012,
Accepted 00th January 2012

DOI: 10.1039/x0xx00000x

www.rsc.org/

A new germanosilicate zeolite (denoted as ITQ-53) with extra-large pores has been synthesised using tri-tertbutylmethylphosphonium cation as the organic structure directing agent (OSDA). Rotation electron diffraction (RED) was used to identify ITQ-53 from an initially-synthesised sample containing impurities, and to solve the structure of ITQ-53 from a micrometer-sized crystal. The structure was refined against PXRD data of pure ITQ-53 samples obtained after synthesis optimisation. ITQ-53 is the first example of extra-large pore zeolites with tri-directional interconnected 14 × 14 × 14-ring channels. It is built from double 3-rings (D3Rs), double 4-rings (D4Rs), and a new composite building unit [$4^2.5^4.6^3$]. D3Rs are very rare, previously only found in two zeolitic silicogermanates. ITQ-53 is stable up to at least 450 °C. The structure of ITQ-53 changes from monoclinic to orthorhombic up on calcination.

Zeolites are crystalline microporous materials with well-defined pores in molecular dimensions. They have wide industrial applications in catalysis, ion-exchange, sorption and separation. These materials can be described as a three-dimensional (3D) framework of vertex-sharing TO_4 tetrahedra, with T atoms being usually Si and/or Al, but also B, Ge, Ti, etc. The spatial distribution and connection of the TO_4 tetrahedra give rise to specific and well-defined systems of channels and cavities, conferring them an important class of materials with interesting applications as molecular sieves and catalysts. Multi-directional extra-large pore (defined by > 12 TO_4 tetrahedra) zeolites are especially interesting, because they can allow large molecules to diffuse in and out of the channels, which facilitates industrial processing of bulky molecules. Despite great synthetic efforts by many groups, zeolites with multi-directional extra-large pore channels are very rare. Among the 225 different zeolite framework types in the Database of Zeolite Structures[1], only three, cloverite **(-CLO)**[2–4], ITQ-37 **(-ITV)**[5] and ITQ-40 **(-IRY)**[6] have multi-directional extra-large pores.

Several approaches have been used to discover new zeolite materials, including the use of ammonium-based organic structure directing agents (OSDAs), and/or inorganic structure directing agents (ISDAs) such as fluoride anions or Ge atoms. In general, large 3D bulky OSDAs may facilitate the synthesis of zeolites with multi-directional extra-large channels. Recently, the use of P-based molecules opened the door to a large family of new OSDAs, for example alkylphosphonium molecules[7–11] and phosphacenes[12].

Zeolites are usually obtained as polycrystalline powders and sometimes with other impurities. When they have large unit cells and complex structures, their structural elucidation by X-ray diffraction becomes extremely challenging. Electron diffraction is a method of choice for structure determination of crystals too small or too complex for X-ray diffraction. One important advantage of electron diffraction is that it can be used to identify new interesting compounds and/or impurities in multi-phasic samples[13,14], which is very helpful for the discovery of new materials. Recently, we have developed a new electron diffraction method, rotation electron diffraction (RED)[15–17], which allows collecting single-crystal-like 3D electron diffraction data from nano- or micrometer-sized particles. It has been used for structure determination of several zeolites[13,18–22]. Here, we present the synthesis and structure of a novel zeolitic structure (ITQ-53) with intersecting three-directional 14-ring channels. We also show the power to combine RED and powder X-ray

diffraction (PXRD) for phase identification and structure determination.

ITQ-53 was obtained using tri-tertbutylmethylphosphonium cations as the OSDA (Scheme 1), and fluoride and GeO_2 as the ISDAs. It was first synthesised at 135 °C as a mixture with another zeolite of the SAS-type framework (Fig. S1, †ESI)[1,23,24]. After ITQ-53 has been identified from the RED data, the synthesis conditions were further improved and pure ITQ-53 samples were finally obtained at 150 °C (Table S1, †ESI). The synthesis gel composition was 0.5 SiO_2: 0.5 GeO_2: 0.5 OSDA(OH): 0.5 HF: 7.0 H_2O. Details about the synthesis of OSDA(OH) and ITQ-53 are given in the ESI S1 and S2. Elemental analysis and ^{13}C MAS-NMR proved that the OSDA remains intact in the framework of ITQ-53 (Fig. S3, †ESI). ^{31}P MAS-NMR suggests that the OSDA may occupy two different locations in the channels, with different interactions between the P atoms and their surroundings (Fig. S3, †ESI). Furthermore, chemical analysis shows that the Si/Ge ratio was 1.1 in the ITQ-53 material (Table S2, †ESI).

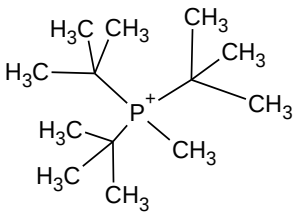

Scheme 1 The organic structure directing agent used for the synthesis of ITQ-53.

PXPD patterns of the initially-synthesised samples could not be indexed due to the presence of impurities. Thus rotation electron diffraction was applied to identify the possible phases in the sample. Transmission electron microscopy (TEM) shows that the samples contain crystals with two distinct morphologies, plate-like and rod-like (Fig. S1, †ESI), which indicates the presence of more than one phase. RED data were collected on crystals with the two different morphologies (Figs. 1 and S5, †ESI). The RED data show that the plate-like crystals have the unit cell a = 19.12 Å, b = 22.77 Å, c = 30.21 Å, α = 90.91°, β = 90.94°, γ = 90.25° (Fig. 1a), which indicates that the crystal is either monoclinic or orthorhombic. The possible space groups are *Cc* (No. 9), *C*2/*c* (No. 15), *Cmc*2$_1$ (No. 36), *C*2*cm* (No. 40) and *Cmcm* (No. 63), as deduced from the reflection conditions of the 2D slices cut from the reconstructed 3D reciprocal lattice of RED data (Fig. 1). Because most zeolite structures in the IZA database are centrosymmetric[1], we performed the structure solution from the RED data by direct methods[25] using the highest centrosymmetric space group *Cmcm*. A partial structure model with ten T atoms (T was assigned as Si in the initial structure solution) and 14 O atoms in the asymmetric unit was established, which form typical zeolite layers with 14-rings (Fig. 3d). In the consecutive refinement, two more Si atoms and six O atoms in the asymmetric unit were located between the layers, which connect the adjacent layers. Four remaining O atoms were added to complete the tetrahedral coordination of the T-atoms between the layers. Further information about the structure solution and refinement are given in ESI S6. The RED data show that the rod-like phase has a body-centred orthorhombic unit cell with a = 14.28 Å, b = 14.00 Å, c = 10.17 Å, α = 90.38°, β = 89.98°, γ = 90.07°. Structure solution from the RED data shows that the framework corresponds to the **SAS** zeolite framework, which was previously reported as a magnesioaluminophosphate (STA-6)[23] and an all-silica zeolite (SSZ-73)[24]. Since the angles determined by RED deviate slightly from 90° (≤ 0.94°) and the deviations are within the error range, we performed a profile fitting on the PXRD data of the initially-synthesised ITQ-53 sample. The results of the profile fitting show that ITQ-53 is monoclinic (a = 18.9248(9) Å, b = 22.8167(10) Å, c = 30.3099(9) Å and β = 90.8819(40)°) and the SAS-type structure is orthorhombic (a = 14.4370(40) Å, b = 14.0966(35) Å, c = 10.2732(53) Å) instead of tetragonal for the ideal SAS framework.

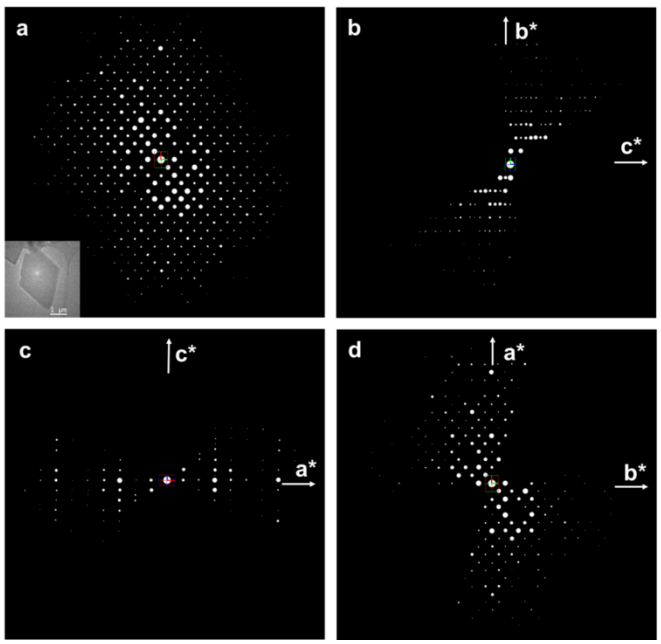

Fig. 1 (a) 3D reciprocal lattice of ITQ-53 reconstructed from the RED data showing *c*-centering. Insert is the TEM image of the crystal from which the RED data was collected. (b-d) (0*kl*) (b), (*h*0*l*) (c) and (*hk*0) (d) planes cut from (a). The reflection conditions can be deduced from the RED data as *hkl*: $h + k = 2n$, 0*kl*: $k = 2n$, *h*0*l*: $h = 2n$ and $l = 2n$, *hk*0: $h + k = 2n$, and *h*00: $h = 2n$. The possible space groups are *Cc*, *C*2/*c*, *Cmc*2$_1$, *C*2*cm* and *Cmcm*.

^{19}F-MAS-NMR spectrum of the as-synthesised ITQ-53 sample shows a single peak at -8.8 ppm (Fig. S4, †ESI), characteristic of fluoride anions in double 4-rings (D4Rs) cages. F^- is commonly found in D4Rs in Ge-containing zeolites[5]. No signal was found that corresponds to F^- in D3R cages, which is in agreement with the results found in the previously known D3R-containing zeolite ITQ-44[26].

In order to obtain a more accurate structure model, Rietveld refinement was performed against the PXRD data of an as-synthesised pure ITQ-53 sample (Cu Kα, λ = 1.5418 Å) using the program *TOPAS*[27]. Because the structure model obtained from RED is orthorhombic, an initial structure model with the monoclinic space group *C*2/*c* was built from the orthorhombic model (the structure transformation was straight-forward since *C*2/*c* is a sub-group of *Cmcm*). Soft restraints on the T-O and O-O distances and rigid body for OSDAs were applied. The final refinement converged to R_B = 1.89%, R_{wp} = 6.86% and R_{exp} = 2.55% (Fig. 2 and Table S5, †ESI). More details about the Rietveld refinement are given in the ESI.

Rietveld refinement was also performed on the PXRD data of a calcined OSDA-free ITQ-53 sample (Cu Kα, λ = 1.5418 Å). The material

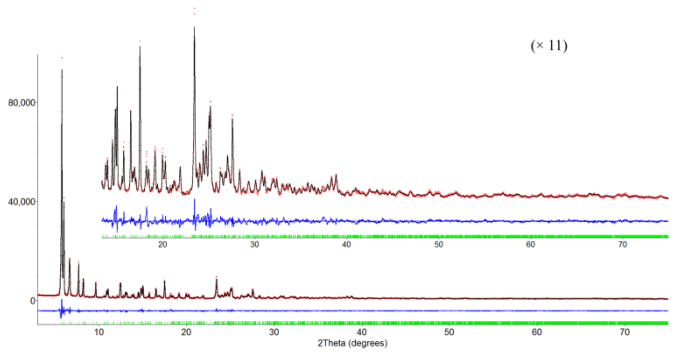

Fig. 2 Observed (red points) and calculated (black) PXRD profiles, as well as the difference between the observed and calculated profiles (blue) for the Rietveld refinement of the as-synthesised pure ITQ-53 (λ = 1.5418 Å). The higher-angle data have been scaled up by 11 times (inset) to show the good fit between the observed and calculated patterns.

was calcined *in situ* in an Anton-Paar XRK-900 chamber attached to the diffractometer at a heating rate of 3 °C/min in a dry air atmosphere. It was kept at 100 °C, 150 °C, 200 °C and 250 °C for 2 hours each, at 300 °C for 8 hours, at 350 °C for 4 hours, and finally at 400 °C for 2 hours. PXRD shows that the structure of ITQ-53 transferred from monoclinic to orthorhombic up on calcination. The unit cell parameters of the calcined ITQ-53 became a = 19.0327(16) Å, b = 22.6345(18) Å, c = 29.252(2) Å. Beside the symmetry change, the c-parameter shrank by ca 1 Å after the calcination. This may be due to the loss of the OSDAs molecules in the pores. Similar changes have been observed in other inorganic frameworks[28,29]. The orthorhombic structure model with space group *Cmcm* obtained from RED was used as the initial model and refined against the PXRD data of the calcined ITQ-53 sample. The residuals of the final refinement converged to R_{wp} = 0.122; R_{exp} = 0.027; R_B = 0.066; R_F = 0.061 (Fig. S6, †ESI S7). The orthorhombic and monoclinic structure models are quite similar, as shown in Fig. S7 (†ESI).

ITQ-53 has a novel 3D framework with extra-large 14 × 14 × 14-ring channels (Figs. 3e-f, Table S9, †ESI). All the 12 T atoms in the symmetric unit are tetrahedrally-coordinated to oxygen atoms, among which 11 are four-connected to other T-atoms and one is three-connected leaving a terminal hydroxyl group. ITQ-53 is built from three composite building units (CBUs): D3Rs, D4Rs and a new CBU [$4^2.5^4.6^3$] containing 16 T-atoms (T = Ge, Si) (Fig. 3a). Each [$4^2.5^4.6^3$] CBU connects to another [$4^2.5^4.6^3$] to form a building unit containing 32 T-atoms (32T) (Fig. 3b). Each 32T building unit connects to other four 32T units via their 4-rings so that a double layer containing 14-rings is formed (Figs. 3c-d). The double layers are connected via D3Rs to form a 3D framework (Fig. 3f). ITQ-53 is the first example of zeolitic materials with tri-directional 14 × 14 × 14-ring channel systems. The 14-ring channels are all straight, along [001], [110] and [1-10], respectively (Fig. S9, †ESI). The 14-ring channel along [001] has a pore aperture of 7.6 × 10.1 Å, while those along [110] and [1-10] have a pore opening of 7.9 × 9.3 Å (after subtracting the diameter of oxygen atoms, 2.7 Å). These values agree with the mean pore diameter found by Ar adsorption (8.1 Å, Fig. S2, †ESI). ITQ-53 has a low framework density of 12.1 T atoms/1000 Å^3. It is the third example of zeolites containing D3Rs, after ITQ-40[6] and ITQ-44[26]. ITQ-53 has a novel zeolite topology, see Table S9 and Fig. S9 (†ESI).

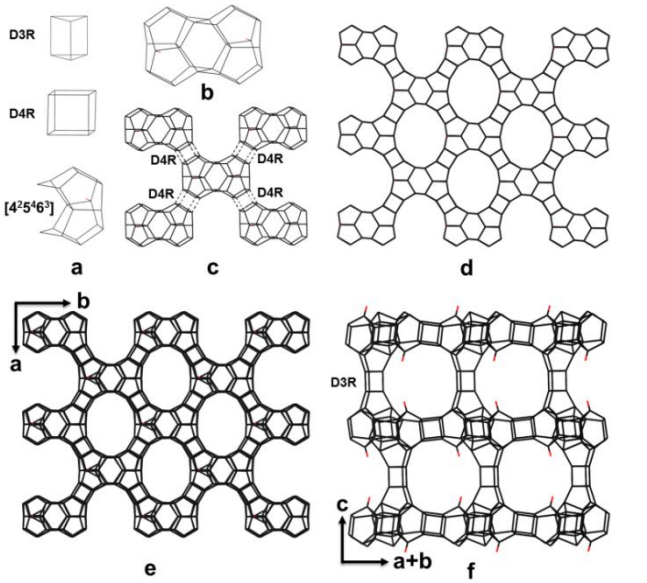

Fig. 3 Construction of the framework structure of the calcined ITQ-53. (a) D3R, D4R, and the new [$4^2.5^4.6^3$] CBU. (b) The 32T unit built from two [$4^2.5^4.6^3$] CBUs. (c) Connectivity of the 32T units. Each 32T unit connects to other four 32T units via D4Rs to form a 14-ring layer in the *ab* plane (d). (e-f) The 3D framework structure of ITQ-53 viewed along (e) [001] and (f) [1-10] directions. The 14-ring layers are connected via D3Rs. Straight 14-ring channels are formed along [001], [1-10] and [110] directions. Only the T-T connections and the terminal OH groups (in red) are shown for clarity.

The 14-ring layer of ITQ-53 is similar to the 14-ring layer of zeolite UTD-1 (**DON**, *Cmcm*, a = 18.890 Å, b = 23.365 Å, c = 8.469 Å)[31] in projection (Fig. 4). However, the orientations of the TO_4 tetrahedra in the layers are very different. In ITQ-53, ten of the 14 TO_4 tetrahedra defining the 14-ring in the layer point to the same direction (down in Fig. 4a). Two such 14-ring layers are connected to form a double layer with very few terminal oxygen atoms pointing outwards. These double layers are further connected via D3Rs to form extra-large 14-ring channels parallel to the layer (Figs. 4b-c). In UTD-1, the 14 TO_4 tetrahedra defining the 14-ring in the layer are oriented up and down in an alternating manner (Fig. 4d). The layers are connected directly without the incorporation of any additional building units. Thus UTD-1 has only 14-ring channel along [001] and does not contain other channels parallel to the 14-ring layer (Figs. 4e-f).

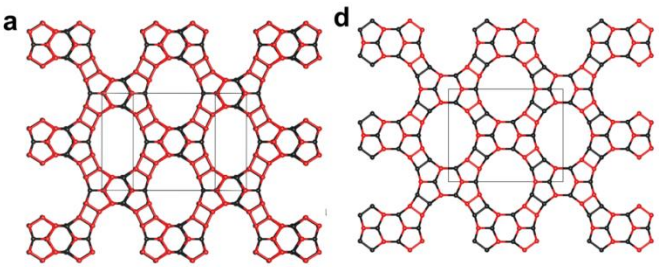

Fig. 4 Comparison of framework structure of (a-c) ITQ-53 and (d-f) UTD-1 (DON), as represented using the T-T connections. The 14-ring layers in (a) ITQ-53 and (d) UTD-1 are similar in projection, but the orientations of the tetrahedra are very different. In ITQ-53, 10 of the 14 TO_4 tetrahedra forming the 14-ring are pointed to the same direction (up: black and down: red); while in UTD-1, the TO_4 tetrahedra are pointed alternatively up and down. In UTD-1, the layers are

directly connected and no channels are formed in parallel to the layers; while in ITQ-53, two layers are connected to form a double layer, which are further connected via D3Rs so that 14-ring channels are formed in parallel to the layers.

In conclusion, the use of tri-tertbutylmethylphosphonium as the OSDA, and fluoride and Ge as ISDAs, allowed the formation of the novel zeolite ITQ-53. ITQ-53 is the first example of extra-large pore zeolites with 14 × 14 × 14-ring pores forming a tri-directional fully interconnected channel system. It contains the unusual D3R cage, previously only found in two zeolitic silicogermanates. ITQ-53 has a permanent pore structure and is stable up to at least 450 °C that allows the removal of the OSDAs in the pores. PXRD shows that the structure of ITQ-53 was changed from monoclinic to orthorhombic up on calcination. We show the power of the RED method in structure solution of micrometer-sized crystals and in discovering new structures in multi-phasic samples. This is important for targeting the interesting materials so that the synthesis conditions can be optimised. We expect that the use of large phosphonium-based molecules can led to more molecular sieves with multi-directional extra-large pore channels, which are essential for processing bulky molecules.

This work was supported by the Spanish Government (MAT2012-38567-C02-01, Consolider Ingenio 2010-Multicat CSD-2009-00050 and Severo Ochoa SEV-2012-0267), the Swedish Research Council (VR), the Swedish Governmental Agency for Innovation Systems (VINNOVA) and the Knut & Alice Wallenberg Foundation through a grant for purchasing the TEMs and the project grant 3DEM-NATUR. Yifeng Yun thanks the China Scholarship Council (CSC).

Notes and references

[a] Berzelii Center EXSELENT on Porous Materials and Inorganic and Structural Chemistry, Department of Materials and Environmental Chemistry, Stockholm University, SE-106 91 Stockholm, Sweden

[b] Instituto de Tecnología Química (UPV-CSIC), Universidad Politécnica de Valencia - Consejo Superior de Investigaciones Científicas, Av. de los Naranjos s/n, 46022 Valencia, Spain

‡ These authors contributed equally to this work.

Email: xzou@mmk.su.se, acorma@itq.upv.es

† Electronic Supplementary Information (ESI) available: Synthesis, textural properties, ^{13}C, ^{31}P and ^{19}F solid state NMR, RED data collection of ITQ-53 and SAS-type zeolites, structure determination by RED, Rietveld refinement against PXRD of as-synthesised and calcined samples of ITQ-53, topology analysis and CIFs. CCDC numbers 1038353 and 1038354. See DOI: 10.1039/c000000x/

1. C. Baerlocher and L. McCusker, Database of Zeolite Structures: http://www.iza-structure.org/databases/.
2. M. Estermann, L. B. McCusker, C. Baerlocher, A. Merrouche and H. Kessler, *Nature*, 1991, **352**, 320–323.
3. J. Su, Y. Wang, J. Lin, J. Liang, J. Sun and X. Zou, *Dalton Trans.*, 2013, **42**, 1360–1363.
4. Y. Wei, Z. Tian, H. Gies, R. Xu, H. Ma, R. Pei, W. Zhang, Y. Xu, L. Wang, K. Li, B. Wang, G. Wen and L. Lin, *Angew. Chem. Int. Ed.*, 2010, **49**, 5367–5370.
5. J. Sun, C. Bonneau, Á. Cantín, A. Corma, M. J. Díaz-Cabañas, M. Moliner, D. Zhang, M. Li and X. Zou, *Nature*, 2009, **458**, 1154–1157.
6. A. Corma, M. J. Díaz-Cabañas, J. Jiang, M. Afeworki, D. L. Dorset, S. L. Soled and K. G. Strohmaier, *Proc. Natl. Acad. Sci.*, 2010, **107**, 13997–14002.
7. D. L. Dorset, K. G. Strohmaier, C. E. Kliewer, A. Corma, M. J. Díaz-Cabañas, F. Rey and C. J. Gilmore, *Chem. Mater.*, 2008, **20**, 5325–5331.
8. D. L. Dorset, G. J. Kennedy, K. G. Strohmaier, M. J. Diaz-Cabañas, F. Rey and A. Corma, *J. Am. Chem. Soc.*, 2006, **128**, 8862–8867.
9. A. Corma, M. J. Diaz-Cabanas, J. L. Jorda, F. Rey, G. Sastre and K. G. Strohmaier, *J. Am. Chem. Soc.*, 2008, **130**, 16482–16483.
10. M. Hernández-Rodríguez, J. L. Jordá, F. Rey and A. Corma, *J. Am. Chem. Soc.*, 2012, **134**, 13232–13235.
11. R. Simancas, J. L. Jordá, F. Rey, A. Corma, A. Cantín, I. Peral and C. Popescu, *J. Am. Chem. Soc.*, 2014, **136**, 3342–3345.
12. R. Simancas, D. Dari, N. Velamazán, M. T. Navarro, A. Cantín, J. L. Jordá, G. Sastre, A. Corma and F. Rey, *Science*, 2010, **330**, 1219–1222.
13. W. Hua, H. Chen, Z.-B. Yu, X. Zou, J. Lin and J. Sun, *Angew. Chem. Int. Ed.*, 2014, **53**, 5868–5871.
14. Y. Yun, W. Wan, F. Rabbani, J. Su, H. Xu, S. Hovmöller, M. Johnsson and X. Zou, *J. Appl. Crystallogr.*, 2014, **47**, 2048–2054.
15. D. Zhang, P. Oleynikov, S. Hovmöller and X. Zou, *Z. Kristallgr.*, 2010, **225**, 94–102.
16. X. Zou, S. Hovmoller and P. Oleynikov, *Electron Crystallography: Electron Microscopy and Electron Diffraction*, Oxford University Press, ISBN: 978-0-19-958020-0, 2011.
17. W. Wan, J. Sun, J. Su, S. Hovmoller and X. Zou, *J. Appl. Crystallogr.*, 2013, **46**, 1863–1873.
18. R. Martinez-Franco, M. Moliner, Y. Yun, J. Sun, W. Wan, X. Zou and A. Corma, *Proc. Natl. Acad. Sci.*, 2013, **110**, 3749–3754.
19. J. Su, E. Kapaca, L. Liu, V. Georgieva, W. Wan, J. Sun, V. Valtchev, S. Hovmöller and X. Zou, *Microporous Mesoporous Mater.*, 2014, **189**, 115–125.
20. P. Guo, L. Liu, Y. Yun, J. Su, W. Wan, H. Gies, H. Zhang, F.-S. Xiao and X. Zou, *Dalton Trans.*, 2014, **43**, 10593–10601.
21. J. Jiang, Y. Yun, X. Zou, J. L. Jorda and A. Corma, *Chem. Sci.*, 2015, **6**, 480–485.
22. T. Willhammar, A. W. Burton, Y. Yun, J. Sun, M. Afeworki, K. G. Strohmaier, H. Vroman and X. Zou, *J. Am. Chem. Soc.*, 2014, **136**, 13570–13573.
23. V. Patinec, P. A. Wright, P. Lightfoot, R. A. Aitken and P. A. Cox, *J. Chem. Soc. Dalton Trans.*, 1999, 3909–3911.
24. D. S. Wragg, R. Morris, A. W. Burton, S. I. Zones, K. Ong and G. Lee, *Chem. Mater.*, 2007, **19**, 3924–3932.
25. G. M. Sheldrick, *Acta Crystallogr. A*, 2008, **64**, 112–122.
26. J. Jiang, J. L. Jorda, M. J. Diaz-Cabanas, J. Yu and A. Corma, *Angew. Chem. Int. Ed.*, 2010, **49**, 4986–4988.
27. R. A. Young, *The Rietveld Method*, Oxford University Press, 1995.
28. H. van Koningsveld, J. C. Jansen and H. van Bekkum, *Zeolites*, 1990, **10**, 235–242.
29. L. Fang, L. Liu, Y. Yun, A. K. Inge, W. Wan, X. Zou and F. Gao, *Cryst. Growth Des.*, 2014, **14**, 5072–5078.
30. V. A. Blatov, *Struct. Chem.*, 2012, **23**, 955–963.

31. T. Wessels, C. Baerlocher, L. B. McCusker and E. J. Creyghton, *J. Am. Chem. Soc.*, 1999, **121**, 6242–6247.